Ocean Engineering
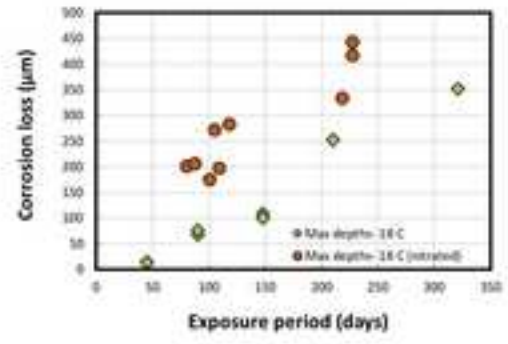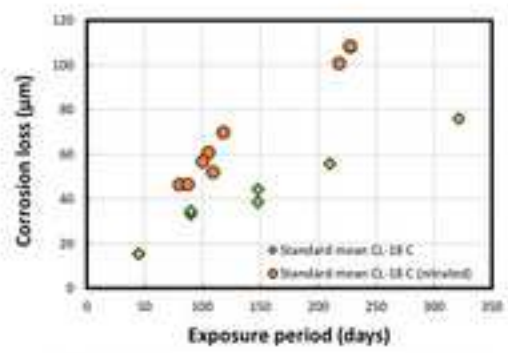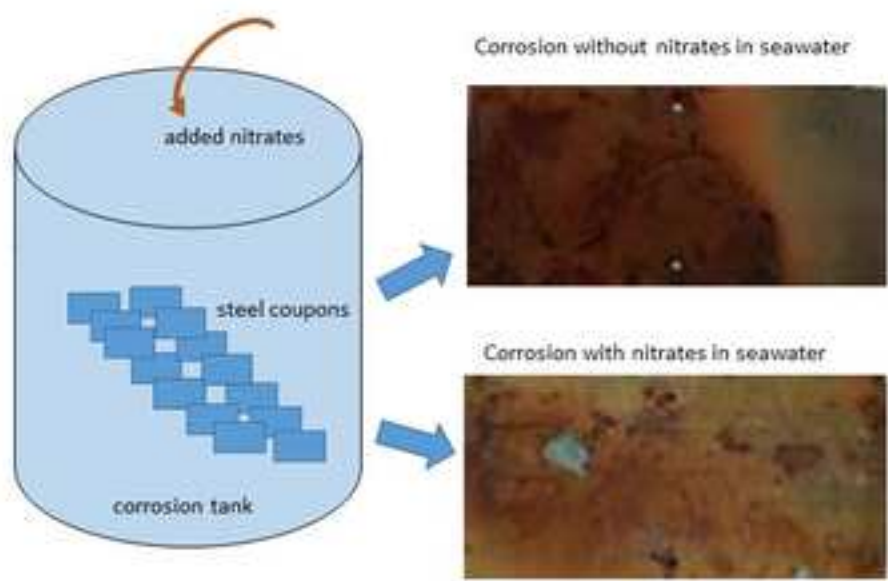
Evaluation of the influence of dissolved nitrates on corrosion behaviour of marine steel exposed to a seawater environment
--Manuscript Draft--

Manuscript Number:	OE-D-23-07304R1
Article Type:	Full length article
Section/Category:	
Keywords:	seawater corrosion; dimensional metrology; artificial seawater; uniform/localised corrosion loss
Corresponding Author:	Muntazir Abbas National University of Sciences and Technology karachi, Sindh PAKISTAN
First Author:	Muntazir Abbas
Order of Authors:	Muntazir Abbas
	Syed Haider Mehdi Rizvi
	Shoaib Sarfraz
	Asif Raza
	Asif Khan
	Adil Loya
	Antash Najib
Abstract:	Corrosion in low carbon steels varies significantly when exposed to seawater bodies at different geographical locations. These structural corrosion variations further intensify in seawaters near harbour or coastal regions, as compared to those exposed to the natural seawater away from shore. Reviewed literature reveals that the accelerated corrosion losses on steels in the polluted seawater may be attributed to the presence of various detrimental chemical species including Dissolved Inorganic Nitrogenous (DINs) compounds, nutrients and sulphur containing compounds, in addition to the interdependent complex relationship between various environmental factors. This paper aims to investigate the influence of nitrate, a DIN compound, on the corrosion behaviour of a low carbon ship structural steel, by exposing surface cleaned coupons to an artificial seawater solution in a controlled laboratory environment. The uniform and localised corrosion damages were measured on steel coupons using the standard weight loss and the dimensional metrology methods. A significant increase in corrosion losses was observed on coupons exposed to nitrate-added artificial seawater than those exposed to similar seawater compositions with no additional nitrate content.
Suggested Reviewers:	Rob Melchers, PhD Professor, The University of Newcastle rob.melchers@newcastle.edu.au
	Nigel Simms Cranfield University N.J.Simms@cranfield.ac.uk
	Zaheer Nasar, PhD Cranfield University Environment and Agrifood z.a.nasar@cranfield.ac.uk

Corrosion without nitrates in seawater

Corrosion with nitrates in seawater

added nitrates

steel coupons

corrosion tank

Evaluation of the influence of dissolved nitrates on corrosion behaviour of marine steel exposed to a seawater environment

Muntazir Abbas[*1,2], Syed Haider Mehdi Rizvi[3], Shoaib Sarfraz[4], Asif Raza[5], Asif Khan[1], Adil Loya[1], Antash Najib[1]

[1]National University of Science and Technology, PNEC, Karachi, Pakistan

[2]School of Water, Energy and Environment Cranfield University, Cranfield, Bedfordshire, MK43 0AL, UK

[3]Queensland University of Technology, Brisbane, Australia

[4]Sustainable Manufacturing Systems Centre, School of Aerospace, Transport and Manufacturing, Cranfield University, Cranfield, Bedfordshire, MK43 0AL, UK

[5]University of Liege, Belgium

Corresponding author email address: Muntazir.Abbas@pnec.nust.edu.pk

Abstract

Corrosion rates in marine structural steels differ significantly with the varying compositions of seawater particularly near harbours or coastal regions primarily due to the presence of untreated chemically active species from various sources. The reviewed literature reports accelerated steels corrosion losses in coastal seawater exposure conditions, which has widely been attributed to the presence of aggressive chemical compounds e.g., dissolved inorganic nitrogenous (DINs) compounds, sulphur containing compounds, in combination with various other environmental factors and their interdependent complex relationships. This paper aims to investigate the influence of nitrate, a DIN compound, on the corrosion behaviour of a low carbon ship structural steel, by exposing surface cleaned coupons to an artificial seawater solution in a controlled laboratory environment. The uniform and localised corrosion damages were measured on steel coupons using the standard weight loss and the dimensional metrology methods. A significant increase in corrosion losses was observed on coupons exposed to nitrate-added artificial seawater than those exposed to similar seawater compositions with no additional nitrate content. Elemental compositions of corrosion deposits and corrosion morphologies investigated using various analytical tools such as SEM, EDS and Raman scattering techniques have shown different types of corrosion products in both artificial seawater exposure conditions.

Keywords: seawater corrosion, dimensional metrology, artificial seawater, uniform/localised corrosion loss

1 Introduction

The potential environmental factors posing a significant influence on the rate of corrosion process of steel structures have been typically categorised into biological, chemical, and physical factors (Aromaa and Forsén, 2016; Soares et al., 2011). The corrosion in seawater submerged steels is a complex phenomenon where chemical interactions between a local environment and steel structures may take place directly or indirectly as a function of exposure duration (Chaves and Melchers, 2014). Steel structures fully or partially exposed to seawater may experience diverse rates of corrosion in seawater compositions at geographical locations, primarily because of the variabilities in corrosion influencing environmental factors (Aromaa and Forsén, 2016; Phull et al., 1997; Venkatesan et al., 2003).

Normally, seawater reservoirs away from harbour or coastal regions contain negligible levels of DIN compounds mainly in the form of nitrates, nitrites, ammonia and ammonium (Melchers and Jeffrey, 2014; Melchers et al., 2016). However, seawater reservoirs contaminated by addition of industrial, agricultural or commercial wastages may contain elevated levels of seawater nutrients including DIN compounds, such as nitrates, nitrites, and ammonia (Kovalenko et al., 2017; Melchers, 2013a). The DIN compounds in form of nitrates, nitrites, ammonia may reach into harbour seawater with the amalgamation of agricultural waste waters from nearby rivers, untreated domestic wastewaters from nearby estuaries and bays, harbour ships/boats (Abbas et al., 2021, 2019a).

Some researchers have reported that the corrosion losses in steels exposed to seawater environment tend to increase significantly with increase in temperature, pollutant levels, and nutrient contents particularly DIN compounds (Chaves and Melchers, 2014; Melchers, 2014a, 2013a). Furthermore, other environmental factors that may significantly influence the rate of corrosion reaction directly/indirectly in seawater submerged steels are: Dissolved Oxygen (DO) concentrations, Sulphide Reducing Bacteria (SRBs), hydrogen sulphide (H_2S), pH, salinity, and flow velocity (Bolwell, 2006; Fanning, 2000; Webster and Newman, 1994).

Some research studies have highlighted that the presence of DINs and other pollutant compounds in seawater influence other environmental factors and overall seawater quality resulting in accelerated corrosion rates in offshore structures (Al-Thubaiti et al., 2005; Melchers and Wells, 2006; Shalaby et al., 2004). Even the presence of lower levels of DINs (0.1 - 1 ppm of nitrogen in nitrate (NO_3-N)) in seawater may result in accelerated corrosion losses in low

carbon steels, and other metal alloys (Jeffrey and Melchers, 2009; Melchers and Chernov, 2010; Melchers and Jeffrey, 2012; Wang and Melchers, 2017).

Accelerated Low Water Corrosion (ALWC) is an aggressive type of microbiologically influenced corrosion (MIC), which typically occur on steel structures exposed to brackish/contaminated seawater regions including harbours and estuarine (Smith et al., 2019). Melchers (2013a) observed that the severity of ALWC in seawater exposed steels is correlated with the concentration of DIN, a crucial nutrient for growth of MIC. A corrosion rate of around 1.0 mm/y has been reported in the ALWC zone having a significant presence of DIN compared to around 0.1 - 0.5 mm/y observed in other corrosion zones in seawater environment. Moreover, Melchers and Jeffrey (2012) found a clear correlation between ALWC of long vertical steel strips and average DIN concentration, in which the latter is considered as an essential nutrient for activation of microbiological activity in seawater environment.

Some researchers consider the relationship between the availability of DIN for microbiological activity, and the rate of corrosion as a more rationalise approach instead of correlating the effect of corrosion rate directly on the microorganisms and their interaction (Melchers, 2014a). According to the reviewed literature, the effect on DIN on the rate of corrosion process is visible only during the long-term corrosion process led by the microbiological activities because the high DIN and nutrients in seawater tends to catalyse the MIC process, hence result in accelerated steel corrosion losses (Melchers, 2018, 2023; Wang and Melchers, 2017). Figure 1 shows short- and long-term corrosion loss modes, modelled for seawater submerged steel as a function of exposure duration. It illustrates the influence of nutrient concentration in natural seawater (in form of DINs) on the corrosion of steels, particularly during the long-term corrosion phase (i.e., anaerobic corrosion) in which corrosion process is controlled by microbiological factors (R. Melchers, 2005; Peng et al., 2017).
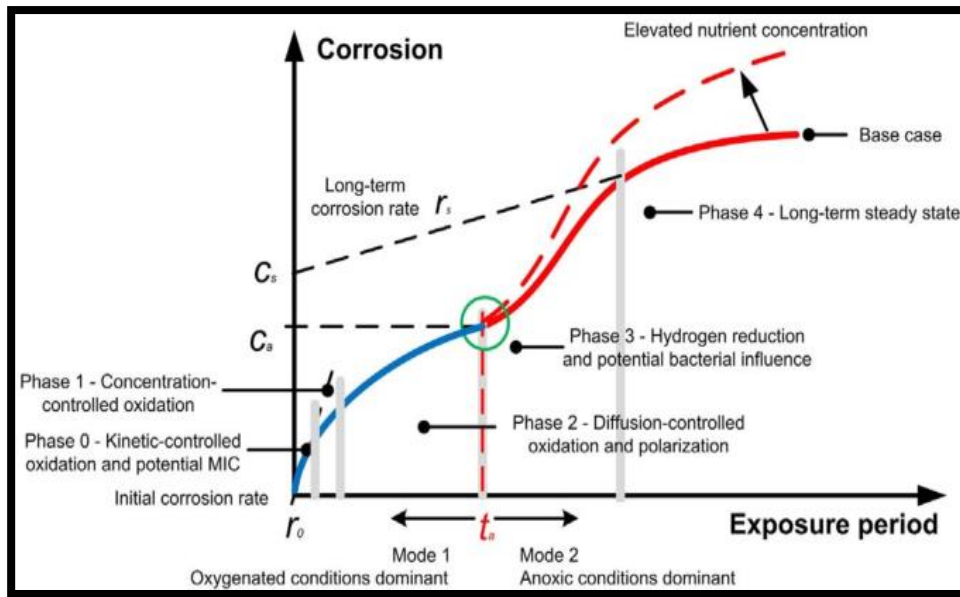
Figure 1 Schematic bi-modal model, showing two modes of corrosion (short- and long-term), and role of nutrient (e.g., DIN) on overall corrosion (Wang and Melchers, 2017)

Nitrate ion is chemically stable in aqueous systems, particularly at lower concentrations, whereas the standard reduction potentials indicate that nitrates serve as an excellent oxidising agent (Fanning, 2000). Some researchers state that the active role of dissolved nitrates toward corrosion process is not just limited to catalysing the growth of biological activities and anaerobic corrosion phases, which typically start during long-term exposures (Melchers, 2014a, 2007a; Wang and Melchers, 2017). During the early diffusion process in the aerobic phase, the diffusion of oxygen through the corrosion layers/deposits (at anodic ends) controls the rate of corrosion reaction (Melchers, 2003). Therefore, permeability, deposition rate, porosity (of corrosion layers developed on steel surfaces) and their corrosion resistance are the most important factors that may vary as a function of alloy compositions in steel, seawater chemistry and pollutant/nutrient levels in seawater (Melchers and Chernov, 2010; Melchers and Jeffrey, 2008; Paul, 2011; Syed, 2010).

The complex interactions between the optimised concentrations of nitrate treatment used for inhibition of SRB activity in offshore steel structures (oil and gas sector) is not a well understood phenomenon. Therefore, contradictory results about acceleration or inhibition of corrosion during nitrate dosing of offshore oil steel reservoirs have been reported by few researchers (Wang and Melchers, 2017). Few research studies have also reported that the addition of lower dose of nitrate sources (5 mM) may not stimulate Nitrate Reducing Bacteria

4

(NRBs); required for inhibiting the growth of SRBs hence it may been concluded that lower doses of nitrate may result in accelerated sour corrosion rates (Pillay and Lin, 2014).

On the contrary to the concept of active role of DINs in elevated corrosion loss in seawater submerged steels, some researchers have reported that the nitrate dosing can be useful to mitigate the sour corrosion risks in offshore oil and gas reservoirs (Gieg et al., 2011; Xu et al., 2013). Hubert et al. (2005) reported that higher dose of nitrate or nitrite (17 mM - 20 mM) successfully reduced sour corrosion by eliminating sulphate; however, it also resulted in elevated localised corrosion. The reduction of nitrates coupled with iron oxidation is thermodynamically favourable, hence under anaerobic condition the NRB may result a significant increase in steel corrosion (Xu et al., 2013).

According to the reviewed literature, it can be ascertained that the influence of DINs on corrosion mechanism in submerged steels is a complex and interdependent phenomena. The active influence of DINs on the overall corrosion of seawater submerged steels has been correlated with the initiation of long-term corrosion process (as shown in Figure 1), which normally takes place under anaerobic conditions led by microbiological activities (Melchers, 2009; Melchers and Emslie, 2016).

Furthermore, few research studies have reported significantly high corrosion losses on steels and cupronickel samples when exposed to DIN-rich seawater in the Arabian Sea region, even after very short exposure durations up to a maximum of 100 days (Abbas et al., 2021, 2019a, 2019b). These studies reported around 4 - 5 times higher corrosion losses on steel and cupronickel alloys exposed to pollutant-rich harbour seawater than those exposed to a clean natural seawater away from the coast. Additionally, high corrosion losses have also been reported by Hubert et al. (2003) and Pillay and Lin (2014) when nitrates were used for inhibiting sour corrosion on steel exposed to oxygenated seawater condition (i.e., aerobic corrosion conditions, typically controlled by concentration/diffusion-controlled oxidation).

The corrosion products that can form on low carbon steels exposed in the marine environments can be made up of various types of oxides, hydroxides, and/or oxyhydroxides existing in the crystalline/amorphous forms (i.e., as compounds of chlorides, sulphates, nitrates, carbonates, etc.). Most common forms of these iron oxide include goethite (α-FeOOH), lepidocrocite (γ-FeOOH), magnetite (Fe_3O_4), maghemite (γ-Fe_2O_3), akaganeite (β-FeOOH), feroxyhyte (δ-FeOOH), hematite (α-Fe_2O_3) and green rust (GR) in form of chloride, carbonates, and sulphates) (Alcántara et al., 2017). These corrosion products mostly occur in crystalline form.

5

In moderate marine climates, the corrosion products deposited onto steel structures are primarily comprised of lepidocrocite, goethite, and magnetite, where the first two forms are found in abundance (Morcillo et al., 2004). Other types of corrosion products including ferrous/ferric chlorides ($FeCl_2$, $FeCl_3$, and $Fe_4Cl_2(OH)_7$), akaganeite and GRs may also appear particularly in the chloride-rich and/or low oxygenated seawater conditions (Refait and Génin, 1997; Rémazeilles and Refait, 2007). Table 1 illustrates typical iron oxide phases and their most probable morphologies (in SEM micrographs).

Table 1 Typical iron oxide phases (Alcántara et al., 2016; Cornell and Schwertmann, 2003)

Oxide	Principal shapes	Other shapes
Goethite	Acicular	Stars, hexagons, bipyramids, cubes, thin/tiny rods, honeycomb, nest-like, feathery, brush-like, cotton balls, sharp edges
Lepidocrocite	Laths	Tablets, thick plates (bent, wiggled), diamonds, cubes, powdery grains, warm packs
Akaganeite	Somatoids, rods	Stars, tubes, crosses (twins), hexagons, prisms
Magnetite	Octahedra, doughnut	Flat dark layers, rhombic dodecahedra, cubes, spheres, bullets, doughnuts
Feroxyhyte	Plates	Needles, sharp plates, flowery crystalline patterns
Ferrihydrite	Spheres	Thick plates (uneven), spindles, cylindrical tubes (e.g., tentacles or cooked spaghetti)

The compactness of rust layers or smaller particle sizes in the rust products often gives greater corrosion resistance. In marine operating conditions, higher porosity in the corrosion layers is more common that acts as voids between larger particles in the corrosion layers and hence accelerate the corrosion phenomena (Alcántara et al., 2017). An irregular, flaked/cracked and non-protective oxide layer permits easy access of corrosive ions/molecules to the metallic substrate whereas, compact oxide layers with closed structures help in the protection of the metallic substrate. (de la Fuente et al., 2011). Roughness on the rust layers is mainly because of the large sized rust particles and their easy fragmentation (Oesch and Heimgartner, 1996). Some researchers have found lepidocrocite as the primary crystalline corrosion product formed during early corrosion of carbon steel (Misawa et al., 1974).

In marine environment, akaganeite is also formed in addition to lepidocrocite primarily due to the presence of higher salinity or chloride (Cl^-) contents. With a rise in the duration of exposure, the rust layer becomes even denser and the lepidocrocite partially transforms into goethite, magnetite/maghemite. Moreover, electrochemical reduction of oxyhydroxides may also results in the formation of magnetite (Rémazeilles and Refait, 2007). Similarly, the reduction of

lepidocrocite in the presence of a low oxygen concentration may also facilitate the formation of magnetite. Similarly, the reduction of lepidocrocite in the presence of a low oxygen concentration may also facilitate the formation of magnetite (Alcántara et al., 2017). Some researchers have found that the formation of magnetite particles may occur due to the reaction of dissolved ferric oxyhydroxides with ferrous species within the solution (Ishikawa et al., 1998; Rémazeilles and Refait, 2007; Tanaka et al., 2014) .

High chloride concentrations also lead to the formation of green rust GR (Cl$^-$) in the inner corrosion layer, which further transforms into more stabilised corrosion products such as lepidocrocite, goethite, akaganeite and magnetite akaganeite (de la Fuente et al., 2016b; Ma et al., 2008). Additionally, presence of akageneite in the near-surface corrosion layers may cause accelerated rates of corrosion (Ma et al., 2008). The formation of magnetite may take place either by electrochemical reduction of akaganeite, and/or lepidocrocite in the oxygen-depleted regions near to the steel surface; even in the absence of Cl$^-$ ions (Alcántara et al., 2016). In the presence of excess dissolved FeCl$_2$, akaganeite can be formed independent of the DO concentration (Rémazeilles and Refait, 2007).

Raman spectroscopy is another powerful, reliable, sensitive and narrow band non-destructive technique, which is widely used for identification and characterisation of oxides, hydroxides and oxy-hydroxides of steels. It can characterise both crystalline and non-crystalline phases (amorphous). Because of the narrower band widths of Raman spectrum, it is ideal for analyses of mixtures or closely occurring peak (Ma et al., 2015; Surnam et al., 2016).

Table 2 shows the characteristic wavelength shift range (cm^{-1}) for Raman peaks for prominent iron oxide phases (de la Fuente et al., 2016a).

Table 2 Characteristic wavelength shifts (cm^{-1}) of the Raman spectra corresponding to corrosion phase location in steels. Underlined wavelength parameters refer to the strongest bands (Cornell and Schwertmann, 2003; Alcántara, et al., 2016).

Compound	Wavelength shifts (cm^{-1})
Goethite	203-206, 241-250, 298-<u>300</u>, 310, 317, 385-<u>386</u>-400, 414-420, 470, 474, 478-485, 549-560, 680-693, 993, 1000-1120
Lepidocrocite	219, 248-<u>252</u>, 301, 311, 349, 378-<u>379</u>–380, 492, 528–532, 638, 650–655, 736, 1300–1310
Akaganeite	310, 312, <u>314</u>, 385–390, 394, 402–410, 415, 420, 497–499, 538–541, 543, <u>549</u>, 607-608, 720–723, 729, 738, 908

Feroxyhyte	297, 385-<u>392</u>-400, 655-665, <u>666</u>–680
Magnetite	298–302, 314, 386, 540–550, 663-<u>667</u>–670
Maghemite	342–350, <u>381</u>, 486, 500–506, <u>670</u>,700–<u>718</u>-720,1400–1440
Ferrihydrite	<u>370</u>, 510, <u>710</u>, 1380–1600
GR (Cl⁻)	160-63, 230-239, 420 425–440, 510–530
GR (SO_4^{2-}, CO_3^{2-})	150, 152, 215–225 255–265, 420, 510

This paper aims to evaluate the influence of a nitrate (a DIN compound) on the early corrosion behaviour of a ship structural steel. Here, simulated artificial seawater solution containing potassium nitrate (KNO_3) is purposefully used (instead of natural seawater) for corrosion experiments, conducted in a controlled laboratory environment, to measure the influence of nitrates on corrosion of steel while negating the influence of other potential corrosion contributing factors such as microbiological agents, which are normally found in the open natural seawater reservoirs. Further, elemental compositions of corrosion products deposited on steel coupons were investigated using SEM, EDS and Raman scattering techniques.

2 Experiment and Methods

The corrosion tests were explicitly designed to evaluate the influence of dissolved nitrates (a DIN compound) on corrosion rate of uncoated and surfaced finished steel coupons exposed to an artificially produced seawater solution at a temperature of 18°C. The corrosion losses and pit depths on steel coupons exposed to nitrated artificial seawater were compared then with those exposed to a similar artificially produced seawater composition without any additional dissolved nitrate content.

2.1 Composition of steel and artificial seawater preparation

In this paper, surface finished uncoated coupons of S-275 steel were used for corrosion tests and material compositions were evaluated using energy dispersive spectroscopy (TESCAN VEGA3), as shown in Table 3.

Table 3 Material composition of experimental steel coupons used during corrosion tests

Fe	C	Mn	Si	Al	Mo
R	0.1	0.34	0.13	0.3	0.2

The steel coupons exposed to the nitrated and the un-nitrated artificial seawater solutions were divided into C-series and J-series for a clear identification of coupons, as shown in Table 4. Furthermore, Table 4 also shows the mean and the standard deviation of seawater temperature

maintained during the corrosion tests, where steel coupons were exposed to artificial seawater for a duration up to a maximum of 321 days in un-nitrated seawater, and up to 227days in nitrated seawater, respectively.

Table 4 Categories of steel coupons exposed to different seawater compositions

Coupon categories (series)	Seawater temperature (^{O}C)	Nitrate content in seawater
C	18 ± 3	un-nitrated seawater
J	18 ± 3	nitrated seawater

The artificial seawater was prepared using a sea-salt mix and tap water (unsterilized) in a laboratory at Cranfield University U.K. The option of using tap water instead of deionised water (sterilised) was adopted because due to the want for relatively large quantity of water (225 litres) to maintain water level in corrosion test rigs, and their frequent replacement needs for retaining the desired quality of artificial seawater solution in each tank. The salinity levels of 40 parts per thousand (ppt.) was maintained by adding approximately 4 kg$_s$ of sea-salt in 100 litres of tap water. This salinity level of 40 ppt. was maintained during the entire duration of corrosion tests, which is equivalent to the maximum salinity levels in the Arabian Sea region (Abbas et al., 2021; Seema Jilani, 2015). Table 5 shows the composition of sea-salt used to prepare the artificial seawater solutions.

Table 5 Composition of sea salt mix (Peacock Salt UK) used to prepare artificial seawater at a concentration of 4 % (salinity level ~40 ppt.)

Chemical compound	Percent composition (%)
Sodium Chloride	66.1
Magnesium Sulphate	16.3
Magnesium Chloride	12.7
Calcium Chloride	3.3
Potassium Chloride	1.6

To simulate the nitrate level of approximately 2 ppm of NO$_3$-N, in artificially prepared seawater, potassium nitrate (KNO$_3$) was added equivalent to 8.85 ppm of Nitrate (NO$_3$), which is equivalent to maximum NO$_3$N content in pollutant-rich seawater in Arabian Sea off the cost of Karachi (Abbas et al., 2021, 2019b). In this research study, the DIN concentration has been represented by the concentration of nitrate content (i.e., NO$_3$-N in potassium nitrate) in seawater.

The seawater quality parameters like seawater temperature, DO concentration, salinity, conductivity, and pH level were maintained and monitored throughout the duration of corrosion experiments with the help of a Multi-meter (HANNA-9128). Non-metallic corrosion tanks (1.8 m^3 capacity) with a seawater temperature controller, water circulation, filtration, and water level control system were used to maintain the desired range of seawater quality parameters including flow velocity.

The mean temperature of seawater tanks was maintained at 18°C and in order to maintain desired DO content in seawater and to inhibit the growth of biological factors the seawater in the tanks was continuously agitated throughout the experimental duration using submersible pumps. Seawater turbidity in the tank was maintained by using a filtration system (with a 5-micron filter), to remove corrosion products which were detached into the artificial seawater with the increasing duration of exposure. The seawater solution was replaced on requirement basis to maintain the predetermined seawater quality parameters, as shown in Table 6. With the continuous agitation of seawater in the tanks, it was assumed that the measured quality parameters were homogenous at all locations and depths in the tanks, and the steel coupons were exposed to similar exposure conditions in the entire duration of corrosion tests.

Table 6 Artificial seawater specifications maintained during the corrosion tests

Parameters	Un-nitrated seawater	Nitrated seawater
Temperature (^{O}C)	18 ± 3	18 ± 3
DO (mg/l)	4.2 ± 0.5	4 ± 0.5
pH	7.7 ± 0.3	7.7 ± 0.3
Conductivity (mS/cm)	60 ± 1.6	60 ± 1.5
Salinity (ppt.)	40 ± 1.3	40 ± 1
Nitrates (NO_3-N in ppm)	Nil	1.5 – 2

2.2 Surface preparation of steel coupons

Each steel coupon was cut into dimensions of 100 mm x 50 mm 3.5 mm and their surfaces were ground to a tolerance limit of 600 UK grit. All pre-exposed coupons were cleaned with deionised water and acetone before exposing to the artificial seawater solutions. Pre-exposure surface preparations, as well as post-immersion mechanical, and chemical cleaning of steel coupons were carried out as per ASTM standard G1-03 (ASTM G1 − 03, 2017), followed by an ultrasonic washing in deionised water. In addition, wire brushes were also used to remove most adherent rust layers from corroded coupon surfaces.

Figure 2 shows the experimental setup, multimeter used to measure seawater quality parameters, pre-exposed surface finished steel coupons and ultrasonic washing rig used during the corrosion tests.
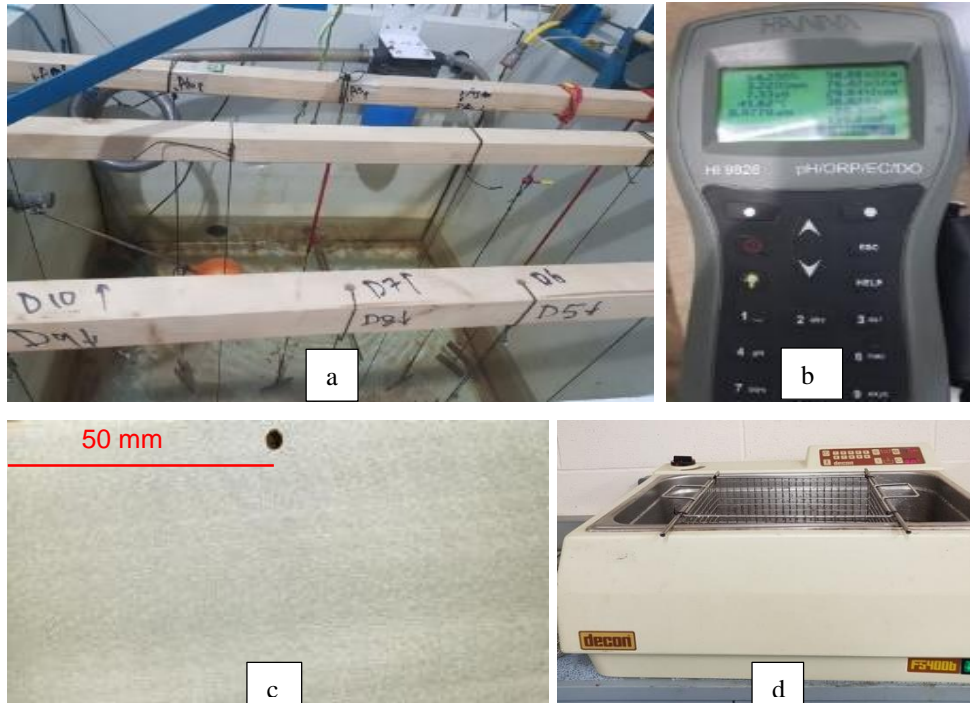

Figure 2 (a) experimental rig (b) multimeter (HANNA 9928) (c) surface finished (600 UK grits) steel coupons (d) ultrasonic washing rig

2.3 Methods for corrosion measurement

In this research corrosion loss measurement has been carried out using a standard average mass-loss (ASTM G1 − 03, 2017; Fontana, 1987), as well as dimensional metrology (DM) methods. The latter has been used for measuring uniform as well as localised metal losses for hot corrosion (Abbas et al., 2021; Simms et al., 2000).

2.3.1 Standard mass loss method

The conventional standard mass loss method was used in this research to calculate the corrosion rates/losses (arithmetic average). A comparative analysis to evaluate the efficiency, as well as limitations with the use of these corrosion measurement techniques has been carried out in the latter part of this research. The values for mean corrosion rates/losses have been calculated with the help of the following equations (ASTM G1 − 03, 2017):

$$C_R \text{ (mm/y)} = 87.6 \text{ x } \left(\frac{\Delta m}{D \cdot A \cdot T}\right) \tag{1}$$

$$\text{Corrosion loss (μm)} = \left(\frac{\Delta m * 1000}{D.\ A}\right) \tag{2}$$

Where C_R is corrosion rate, Δm is the mass difference (in mg) prior/post immersion, D is the density (in grams/cm^3), A is the surface area of coupons (in cm^2) and T is the exposure duration (in hours). Here, the corroded coupons collected after each exposure time were reweighed and difference in the mass was calculated, followed by the evaluation of corrosion rates/losses, using equation ((1) and equation (2). Density of 7.85 g/cm^3 has been taken for all steel coupons.

2.3.2 Dimensional metrology (DM) – micrometry method

The DM-micrometry approach is primarily based on measurement of steel coupons dimensions at pre-determined thickness positions before and after their exposure to the artificial seawater. In this paper, the pre-exposure contact metrology of coupon dimensions was carried out using a Mitutoyo digital micrometer (with rounded tips for measuring pit depths) with a resolution of ±1 μm. Post-corrosion coupon thicknesses at predetermined positions and their immediate vicinities were measured again with micrometer. Figure 3 shows a typical pattern for measuring corrosion depths at various locations on steel coupons.
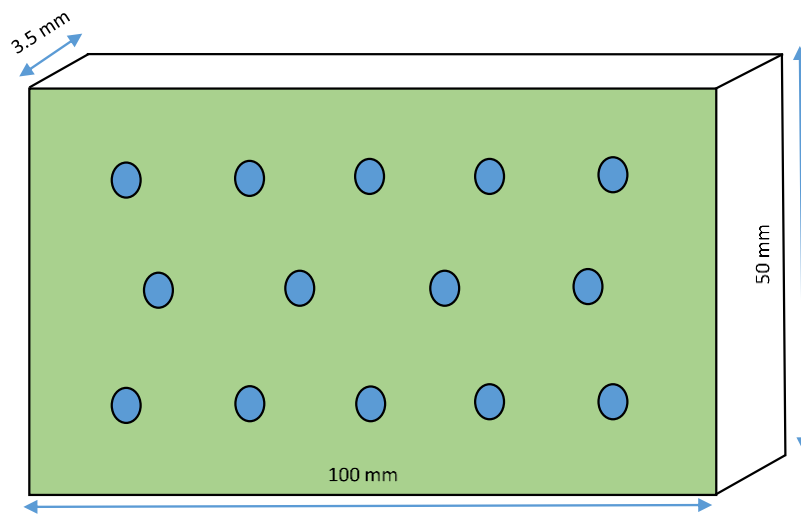

Figure 3 Schematic of the DM-micrometry pattern for measuring thickness losses across coupon surfaces. The shaded dots indicate the positions measured for metal thickness (Abbas et al., 2023)

The cumulative probability (%) of thickness loss data on steel coupons was plotted (in results section) and various statistical parameters of the corrosion loss data were evaluated for coupons exposed both to the nitrated and un-nitrated artificial seawater solutions. Here, cumulative probability (%) was determined using following equation:

$$cumulative \; probability \; (\%) = \frac{n}{N+1} \; X \; 100 \qquad (1)$$

Where 'n' is rank number and 'N' is total number of thickness loss points on each steel plate. For further details of the DM-micrometry method, and cumulative probability (%) thickness loss measurement using reader are referred to the research paper of (Abbas et al., 2023).

3 Results

3.1 Corrosion measurements

The corrosion losses on steel coupons were evaluated on C-series steel coupons, after their immersion in an un-nitrated artificial seawater for various durations up to a maximum of 321 days. Figure 4 shows maximum pit depths and mean corrosion loss parameters calculated using DM-micrometry and standard mass loss methods.
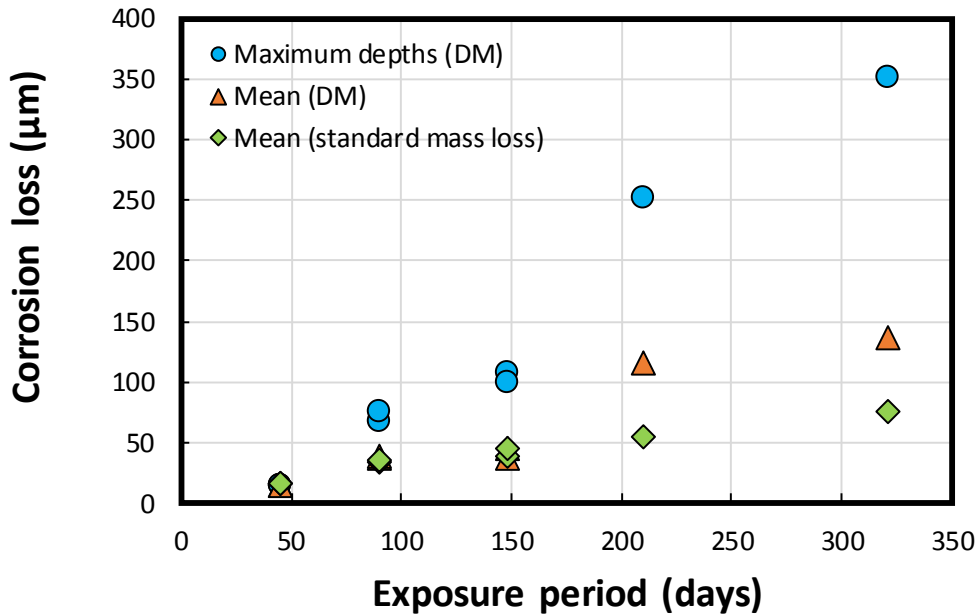
Figure 4 Corrosion loss parameters calculated for steel coupons (C-series) exposed to the un-nitrated artificial seawater

Likewise, the corrosion results observed on steel coupons (of similar material dimensions and surface finishing) immersed in a nitrated artificial seawater solution, for a duration of up to a maximum of 227 are shown in Figure 5.
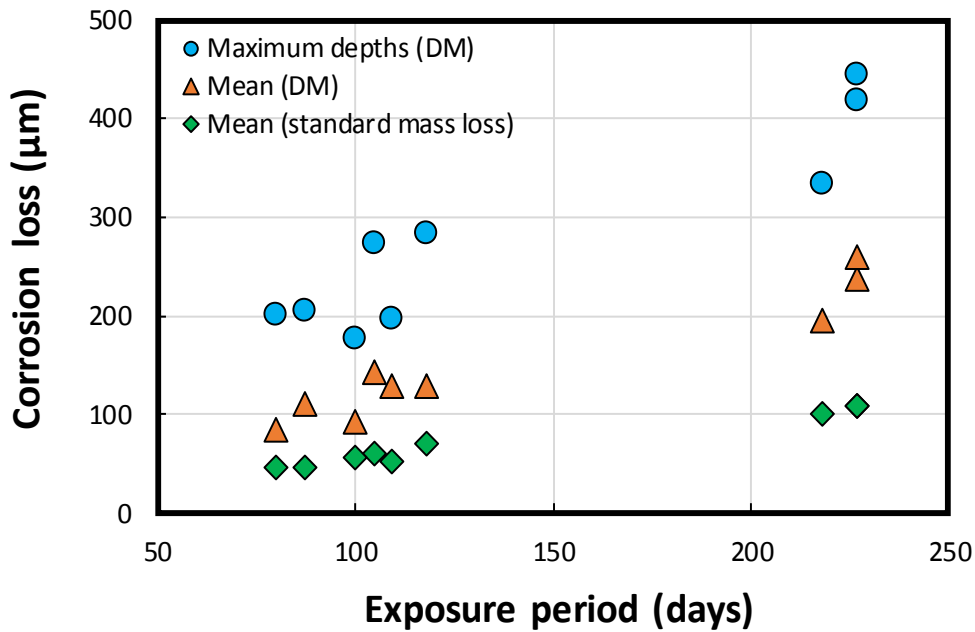
13

Figure 5 Corrosion loss parameters calculated for steel coupons (J-series) exposed to nitrated artificial seawater

Overall, the corrosion loss patterns shown in Figure 4 and Figure 5 show that the maximum corrosion depth and the mean corrosion loss parameters (calculated using both DM-micrometry and standard mass loss methods) were found to be considerably higher in case of steel coupons exposed to the nitrated artificial seawater.

Additionally, Figure 6 and Figure 7 show the comparative graphs for mean corrosion loss and maximum depths on steel coupons, exposed to the nitrated artificial seawater (J-series) and the un-nitrated artificial seawater (C-series), respectively. These loss parameters were then calculated using the standard mass loss and the DM-micrometry methods. The mean corrosion rates were ranged between 0.33-0.42 mm/y when exposed to nitrated artificial seawater for a duration up to a maximum of 227 days, whereas for similar duration it ranged between 0.1-0.15 mm/y in a seawater medium without nitrate content.
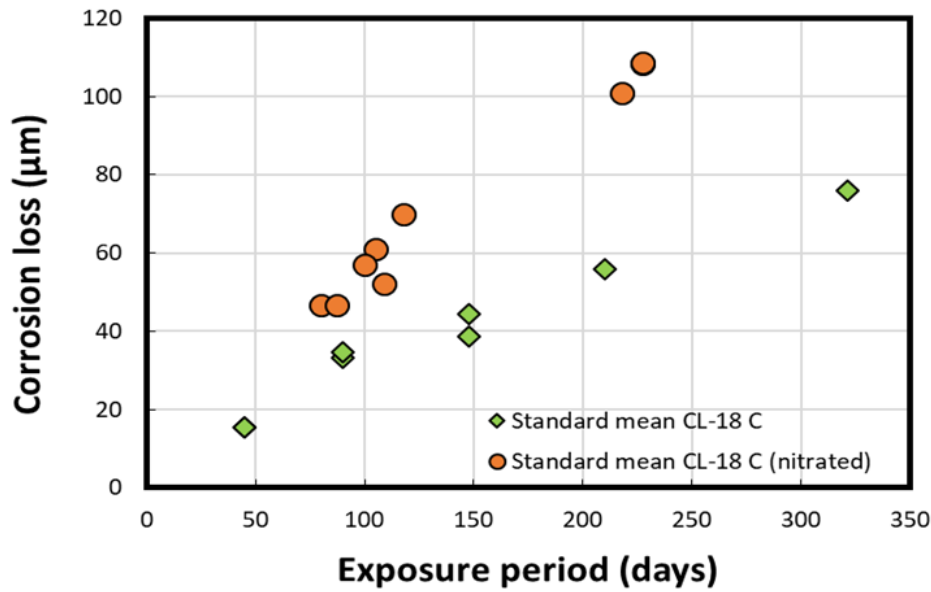
Figure 6 Comparison of mean corrosion losses observed on steel coupons exposed to the nitrated artificial seawater (J-series) and the un-nitrated artificial seawater (C-series), and calculated using standard mass loss method. Here 'CL' indicate corrosion loss
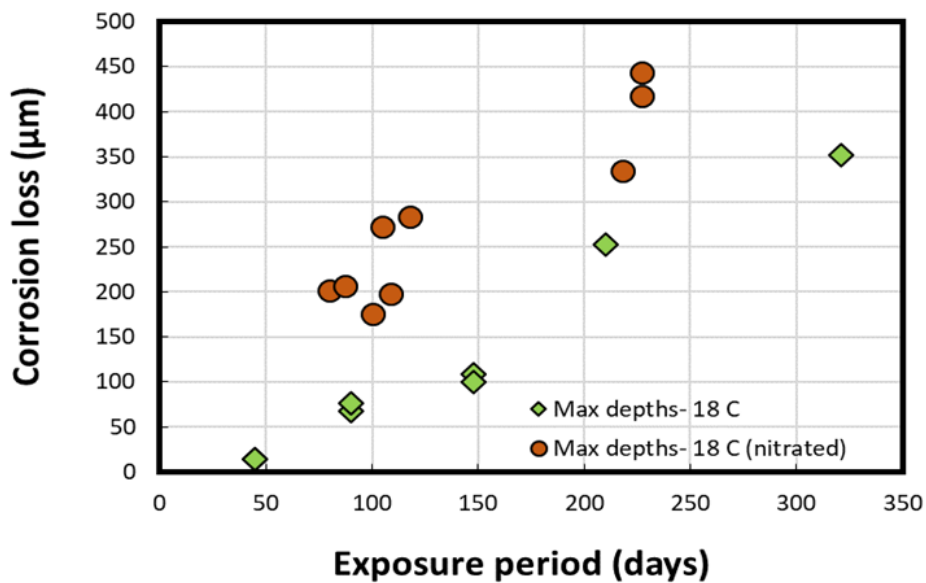

Figure 7 Comparison of maximum corrosion depths observed on steel coupons exposed to the nitrated artificial seawater (J-series), the un-nitrated artificial seawater (C-series), and calculated using DM-micrometry method

The cumulative probability (%) of corrosion loss data for the C-series and J-series steel coupons, and calculated using the DM-micrometry technique are shown in Figure 8 and Figure 9, respectively.
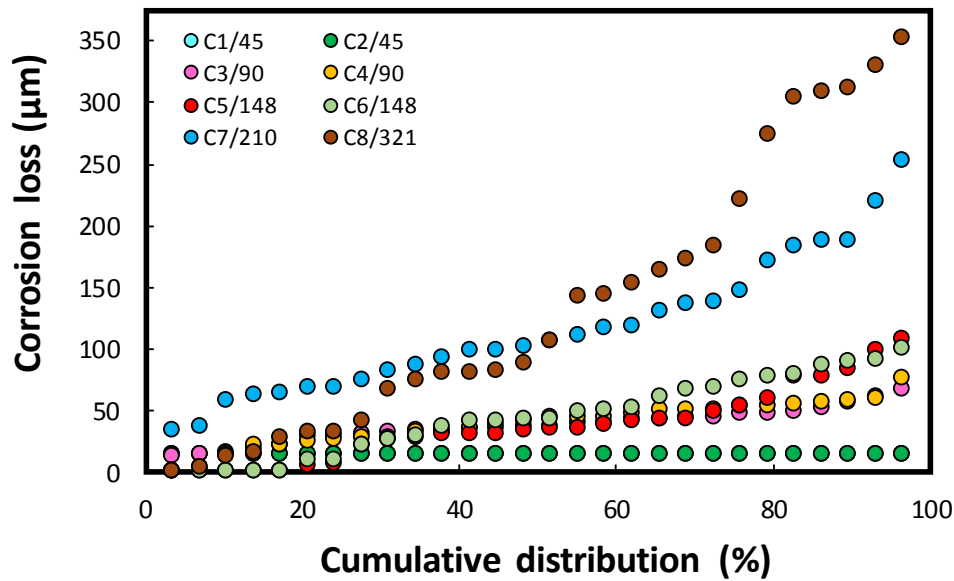
15

Figure 8 Cumulative probability distribution (%) of corrosion losses on C-series steel coupons exposed in artificial seawater. Here, C indicates the name of steel coupon and the number after slash shows exposure durations (in days)
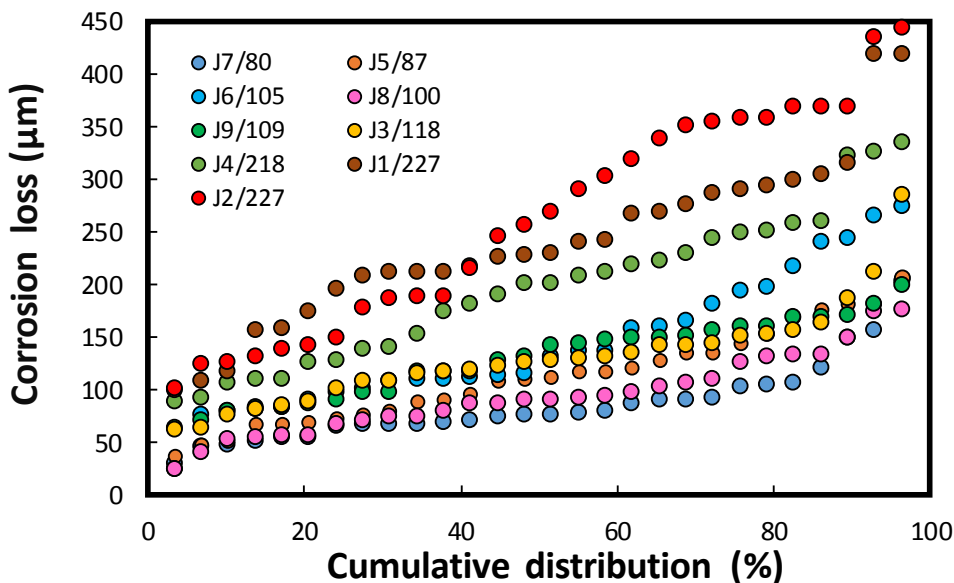

Figure 9 Cumulative probability distribution (%) of corrosion losses for J-series steel coupons exposed to the nitrated artificial seawater. Here, J indicate the name of steel coupon and the number after slash shows the duration of exposure (in days)

In Figure 8, the cumulative probability (%) of corrosion losses for C-series steel coupons remained quite low and steady up to 148 exposure days however, an elevated trend of corrosion depths was observed beyond this period (maximum depths ranging 0.25-0.35 mm were observed between 200-321 exposure days). Similarly, in J-series steel coupons exposed to

16

nitrated seawater solution (in Figure 9), the maximum corrosion depths ranged between 0.4-0.45 mm after maximum exposure duration of 227 days. Similar to the corrosion trend in un-nitrated seawater, here (Figure 9) the rapidly increasing trend of corrosion depths is more significant after first 200 exposure days.

Overall, Figures 6-9 indicate that the mean corrosion losses and maximum depths were found to be significantly higher on steel coupons exposed to the nitrated artificial seawater (for a maximum duration of 227 days), than those exposed in similar seawater compositions (un-nitrated), even after exposure for extended durations of up to a maximum of 321 days. Most importantly, one of the limitation being experienced during the laboratory based corrosion experiments (at Cranfield University U.K), where the maximum exposure duration of steel coupons (J-series) dipped in nitrated seawater could not extended beyond 227 days because of the lockdown situation due to COVID-19 and safety practices adhered in research laboratories.

3.2 Morphologies of deposited corrosion products

Figure 10 shows the macrographs of the corroded steel coupons of C-series, exposed to the un-nitrated artificial seawater at 18°C. The cathode regions were protected by a hard greyish protective layer which remained intact throughout the exposure period. On the coupons collected after 250 days of exposure, the protective layers developed on the cathode regions were hard enough that they could not be removed completely even after chemical cleaning and mechanical brushing.

Figure 10 Pictorial view of the corroded and chemically cleaned steel coupons (C-series) collected from artificial seawater. Here exposure periods are as follows: (a, b) 45 days (c, d) 90 days (e, f) 210 days and (g, h) 321 days

17

On the anodic regions, a powdery, soft, and bright reddish/orange coloured corrosion deposits were formed at a slower rate, which possibly represents the unstable lepidocrocite phase. Further, on these coupons, the innermost corrosion layers (near metal surface) did not turn into blackish oxides for the first 150 days, however, the blackish layers were observed on the coupons collected after 210 and 321 days of seawater exposure.

Similarly, Figure 11 shows a pictorial view of the post-corrosion as well as cleaned well pre-corrosion steel coupons of J-series exposed to the nitrated artificial seawater (at 18^OC).
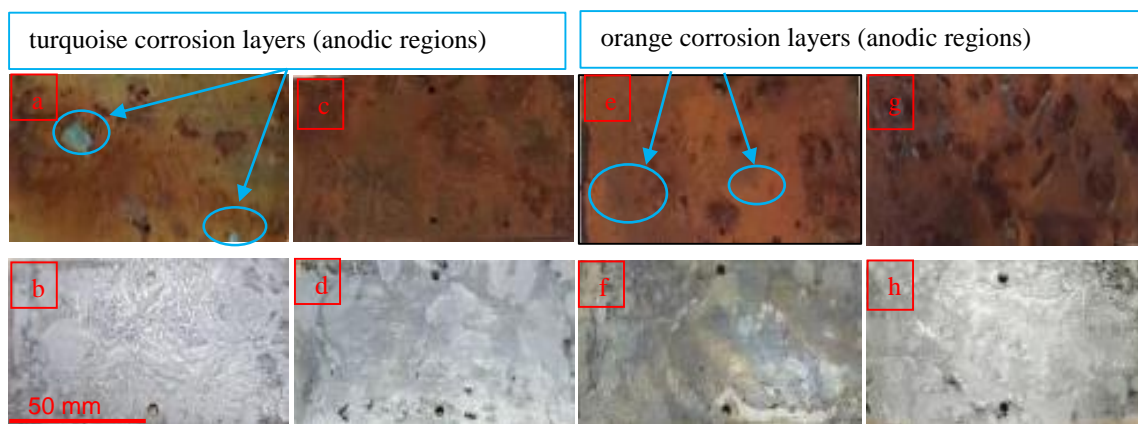

Figure 11 Corroded and chemically cleaned steel coupons (J-series) recovered after 80 - 227 exposure days in the nitrated artificial seawater. Here exposure periods are as follows (a, b) 118 days (c, d) 80 days (e, f) 87 days and (g, h) 227 days

Here in Figure 11, relatively larger anodic regions covered with a powdery, soft, and orange-reddish corrosion product (probably lepidocrocite phase) were observed that transformed into a dark brown shade with increasing exposure time. The corrosion layer close to the steel surfaces turned mostly into a blackish (magnetite), and greenish/turquoise coloured rust layers (under the exfoliated reddish rust), particularly after the longer exposure durations (beyond 150 days). Contrary to the hard and protective type of corrosion deposits observed on coupons immersed in the un-nitrated seawater (as shown in Figure 10), the corrosion deposits resulted in the nitrated seawater solution were easily peelable and non-adherent to the coupon surfaces.

In addition to the visual microscopy of the post-corrosion coupons, characterisation of the corrosion deposits on post-corrosion steel coupons by using various analytical techniques (e.g., SEM, EDS and Raman scattering) provide useful information and correlations between the corrosion rates and elements in various corrosion layers. Figure 12 shows SEM micrographs of corrosion products collected from anodic regions of C-series (except Figure 12a) steel coupons exposed in un-nitrated artificial seawater. At lower magnification, the structures

18

resemble clusters of rectangular-shaped rods (bent and twisted). Whereas, at the higher magnification of 20kx, circular spongy plate type morphologies are also visible along with the lath-shaped thick rods or plates. These SEM morphologies have resemblance to lepidocrocite, goethite, and akaganeite (Alcántara et al., 2016; Cornell and Schwertmann, 2003). Further, Figure 12a shows SEM micrograph for corrosion deposits collected from cathode regions (as shown in Figure 10) of steel plate after 321 exposure days.
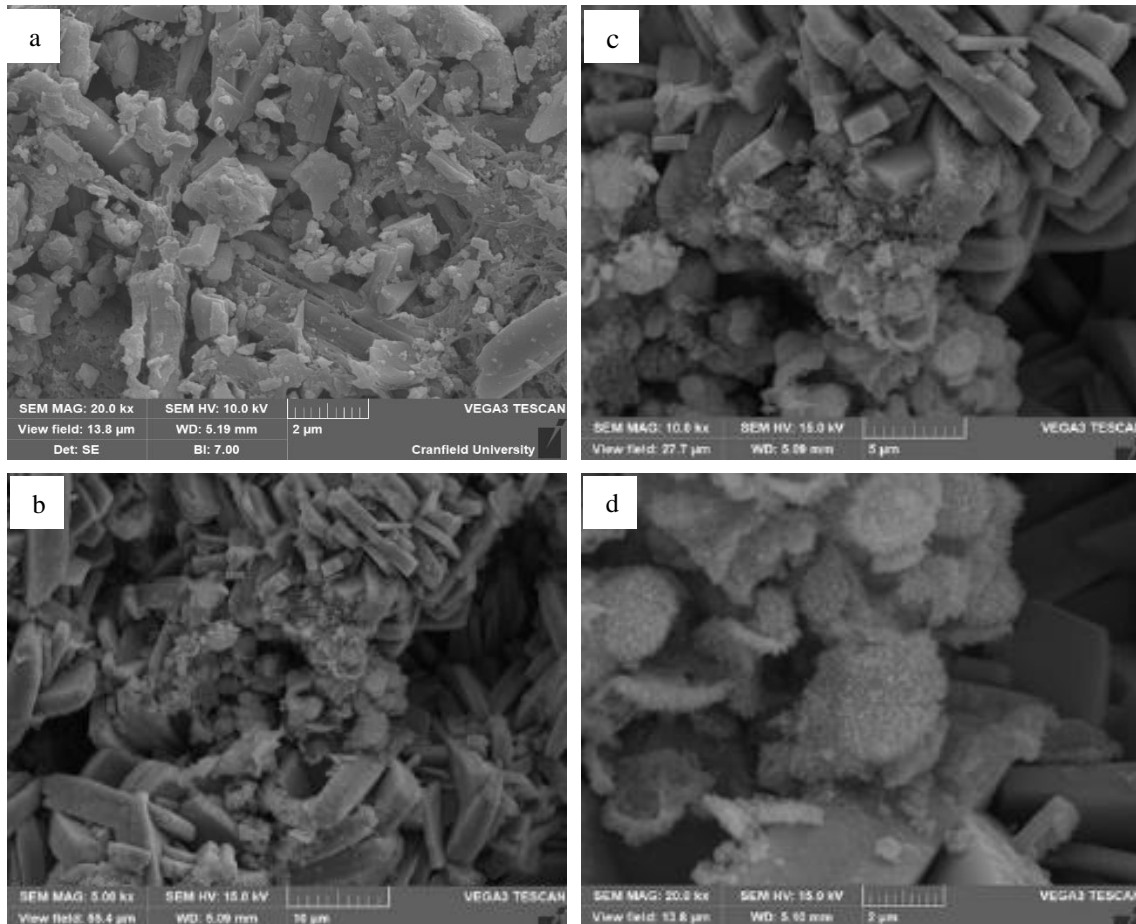
Figure 12 SEM micrographs of the corrosion products (at various magnifications) recovered from C-series coupons after 321 days of immersion in artificial seawater. Here, (a) protective coating on cathode regions of steel coupons (b) 5kx (c) 10kx (d) 20kx, respectively.

EDS results along with the relevant low magnification micrographs, and detailed elemental compositions for corrosion products on C-series steel coupons are shown in Figure 13, and Table 7. No significant presence of corrosion-sensitive elements (such as S, and Cl) was observed in EDS curves.
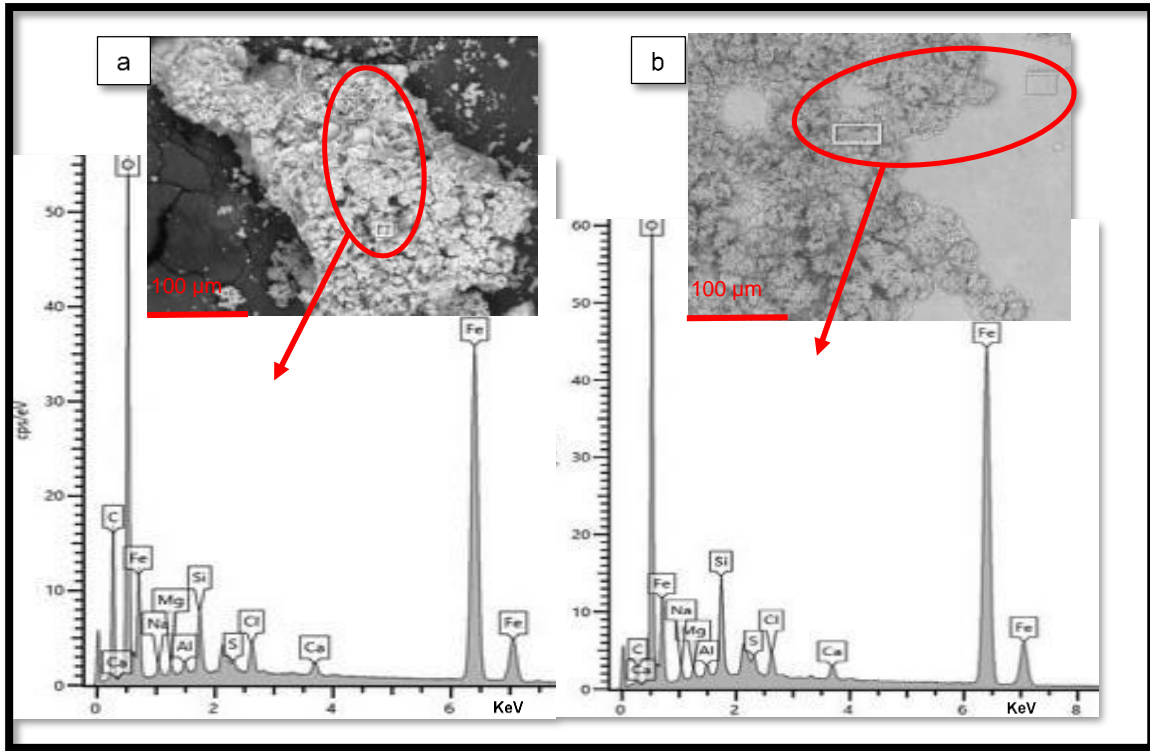
19

Figure 13 EDS results for corrosion products collected from anodic regions of C-series steel coupons immersed in artificial seawater for 321 days

Table 7 Elemental compositions (wt. % evaluated using EDS) for corrosion products recovered from C-series steel coupons for 321 days

C	O	Na	Mg	Al	Si	S	Cl	Ca	Fe
27.7	41.6	0.6	0.3	0.2	1.2	0.2	0.8	0.4	26.7
7.9	39	0.8	0.4	0.4	3.0	0.6	0.8	0.6	46.2

Furthermore, EDS results for corrosion deposits collected from cathode regions (as shown in Figure 10) of steel plates after 321 exposure days showed significantly different compositions than those shown in Table 7. Here in Figure 14, the protective deposits on cathode regions were mostly comprised of Ca (32 wt.%), O (64 wt.%), and Fe (2 %), which may probably show $CaCO_3$ compounds.
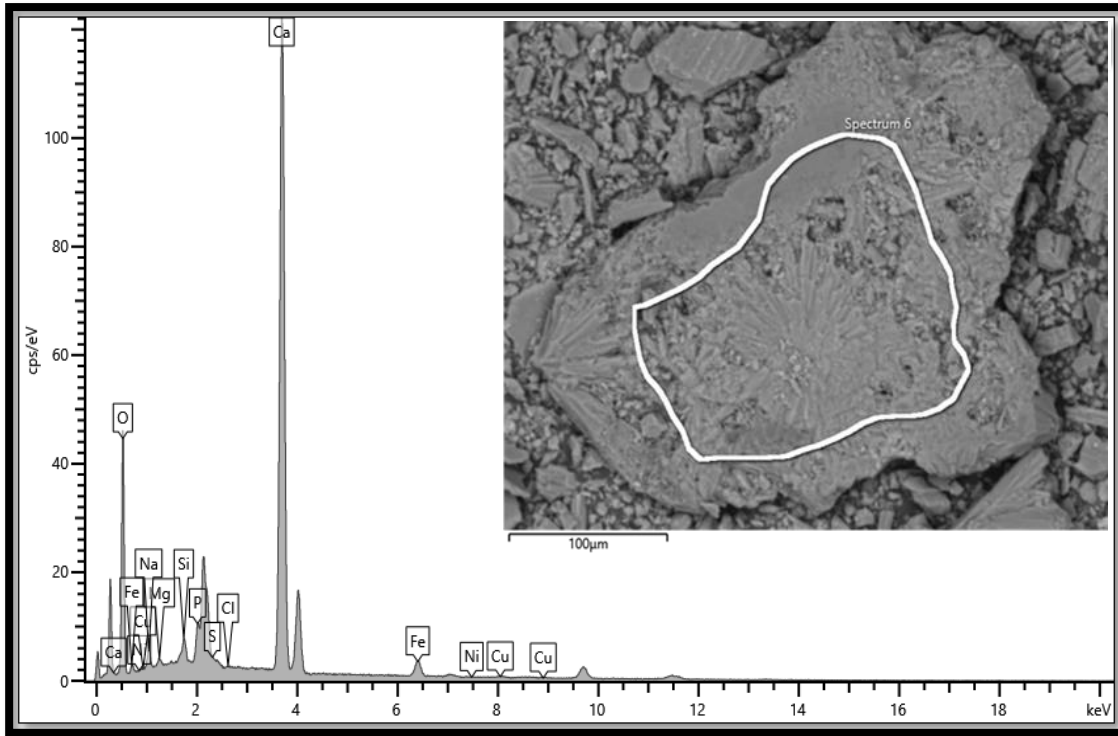
Figure 14 EDS results for corrosion products collected from cathode regions of C-series steel coupons immersed in artificial seawater for 321 days

The Raman spectrum in Figure 15 comprises peaks belonging to probable bands of goethite at 482, 1052 cm^{-1}, lepidocrocite at 383,639, 654 cm^{-1}, akaganeite, or magnetite at 383-6 cm^{-1}. The presence of the ferrihydrite phase is also possible at 385 and 654 cm^{-1}. The strong band at 111 cm^{-1} may probably represent a $CaCO_3$ compound.
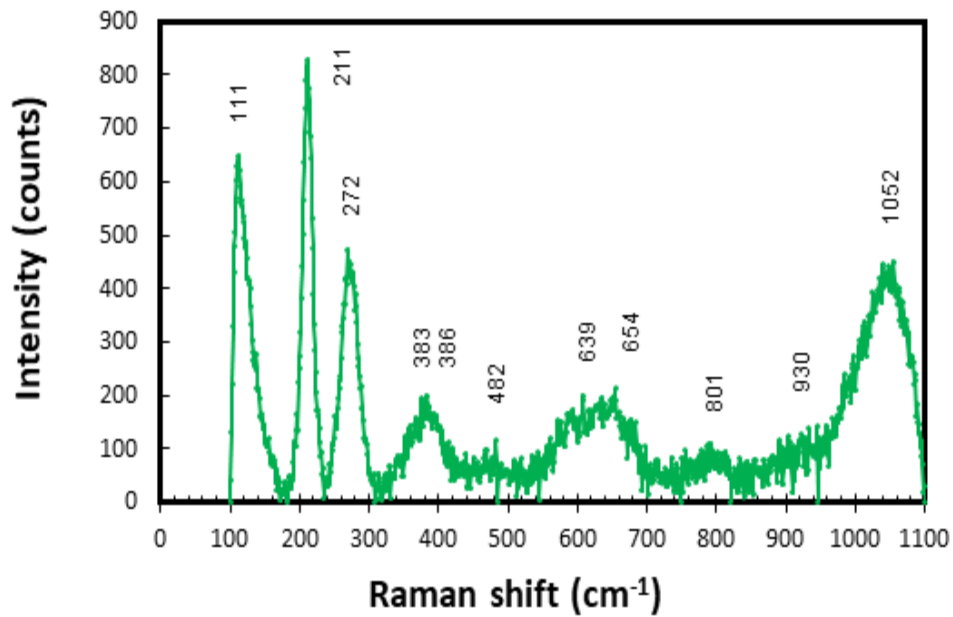
Figure 15 Raman analyses on rust product collected from C-series steel coupons exposed in un-nitrated artificial seawater (321 days)

In J-series steel coupons exposed to nitrated artificial seawater for 227 days, the SEM micrographs for corrosion deposits are shown in Figure 16, which mainly comprised of rod type structures, sponge type, cotton balls and thin tiny rod morphologies with spongy shapes. These shapes are commonly attributed to akaganeite (rods) and goethite (spongy, cotton ball and tiny rods) phases. Additionally, the tiny rods with the shape of cooked spaghetti are also visible in the spaces between the cotton balls, which may also be attributed to the ferrihydrite structures (Table 1). Some uneven disc-shaped, brush-like, and circular rod-shaped crystalline structures are also visible (at 10 - 20 kx), mutually belonging to ferrihydrite, lepidocrocite, goethite, and akaganeite phases, respectively.
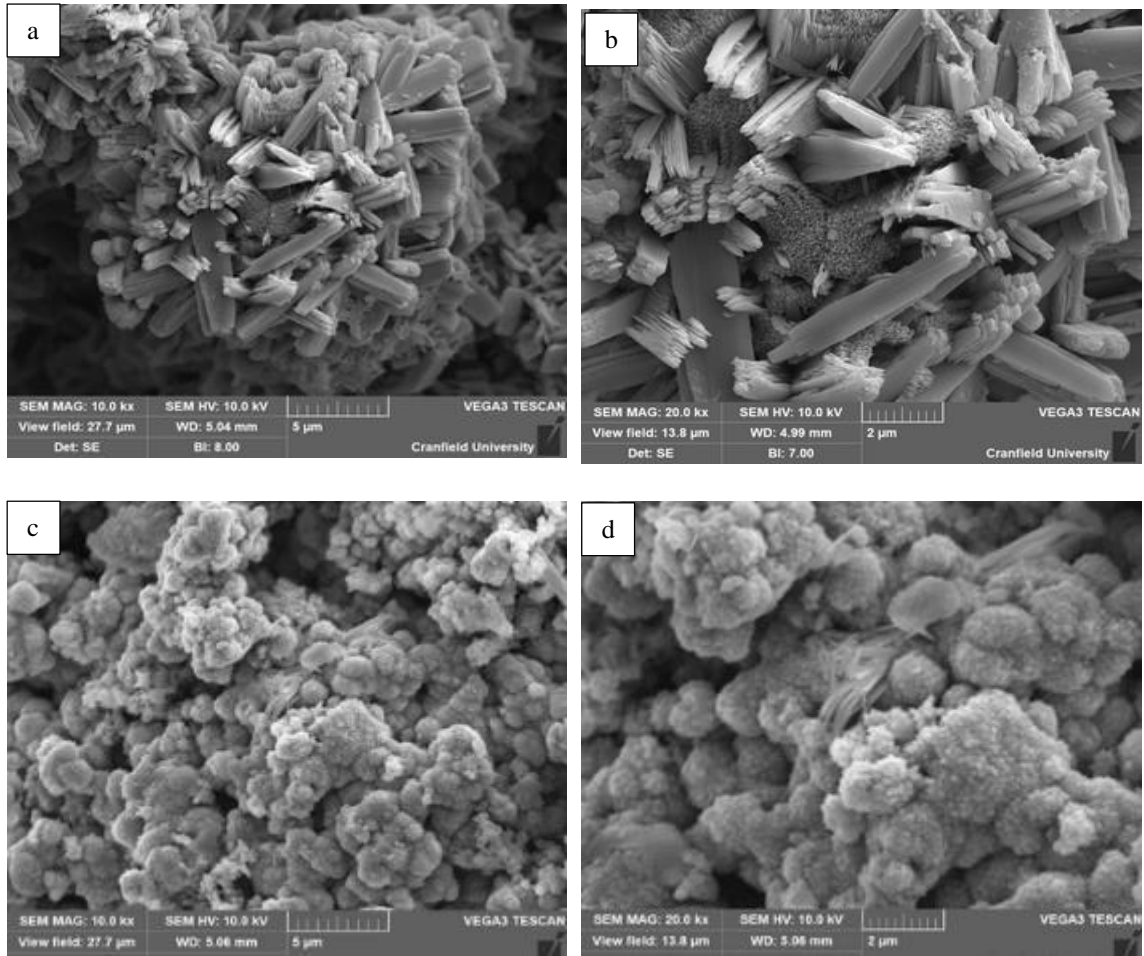
Figure 16 SEM micrographs (at 10kx and 20kx) of corrosion product from J-series steel coupons recovered after (a, b) 105 days (c, d) 227 days of immersion in nitrated artificial seawater

The EDS plot and elemental compositions of various corrosion deposits from J-series steel coupons after 227 days of immersion in nitrated artificial seawater are given in Figure 17 and Table 8. Further, no protective (cathode) regions appeared on coupons (J-series) exposed to nitrated seawater.
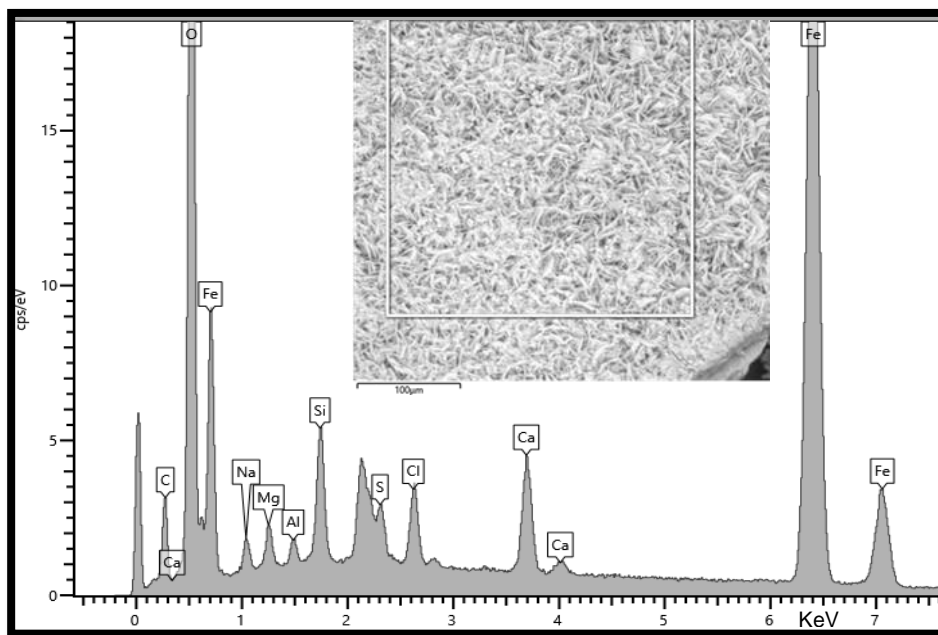
Figure 17 EDS of corrosion products collected from J-series steel coupons after 227 days of immersion in nitrated artificial seawater

Table 8 Elemental compositions (wt.%) of the corrosion products (evaluated using EDS on several carrion deposits) recovered from J-series steel coupons after 227 days in the nitrated artificial seawaters

C	O	Na	Mg	Al	Si	S	Cl	Ca	Mn	Fe
14.6	35.8	1.3	1.2	1.8	1.3	0.9	0.9	1.8	0.2	39.8
17.4	38.7	1.71	1.4	1.9	1.3	1.3	1.0	2.5	0.3	32.6
-	46.6	3.3	0.45	-	0.23	2.16	2.66	1.27	-	43.2

The Raman scattering plots of two samples of corrosion products are shown in Figure 18. Some prominent peaks are matching the strong bands of typical iron oxide phases such as: goethite at 203, 422, 1055-59 cm^{-1}; lepidocrocite at 355, 655 cm^{-1}; GR (Cl, SO$_4$) at 261, 354, 422 433, 511 cm^{-1}, magnetite, and akaganeite can also be expected at 544 cm^{-1}; whereas 657 cm^{-1} comes near the strong bands of magnetite. The strong band at 106-109 cm^{-1} may probably represent a CaCO$_3$ compound, whereas peaks between 511-515 cm^{-1} range in the most probable band for the ferrihydrite phase.
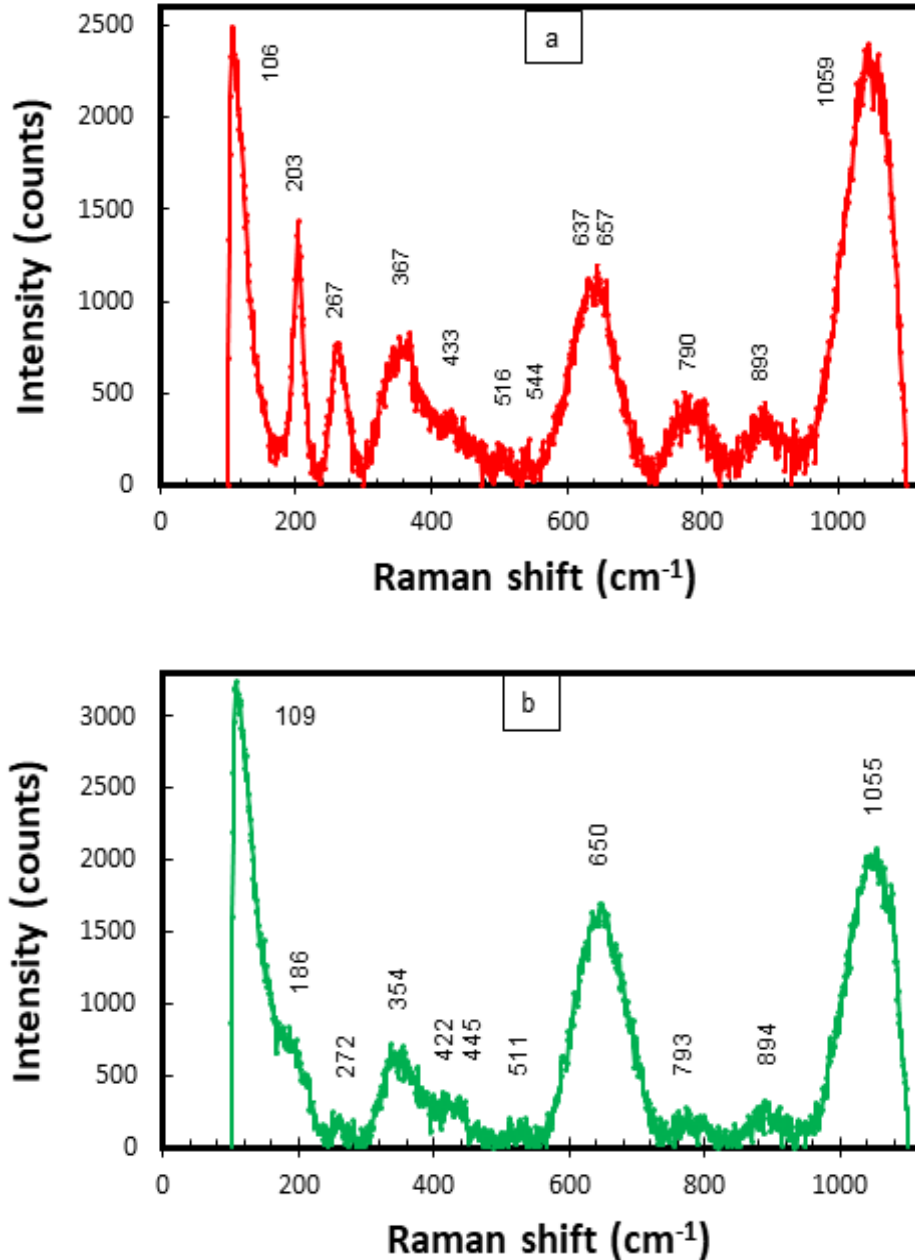
Figure 18 (a, b) Raman scattering plots for corrosion products collected from steel coupons (J-series) after 227 days in nitrated artificial seawater solution

4 Discussion

In this study, the corrosion test results revealed that the presence of dissolved nitrates in the oxygenated artificial seawater (at 18^OC) may significantly influence the corrosion process by elevating the corrosion rates/losses. These results have also indicated that the nitrates added (1.5-2 ppm of NO_3-N) in the oxygenated artificial seawater may act as oxidising agents and tend to increase the rate of corrosion reaction even in the preliminary activation/concentration

polarisation stages, by stimulating oxidation reaction at anode and reduction reaction at the cathode (as shown in Figures 4 - 8).

These corrosion test results conducted for short durations (less than one year) in an artificial seawater medium at 18 ^{O}C show that a slight increase in dissolved nitrate levels in seawater (around 1.5–2 ppm NO_3-N) may significantly increase corrosion losses taking place in the kinetic- and concentration-controlled oxidation (i.e., aerobic conditions). Even higher corrosion trends have been previously reported by Abbas et al. (2021, 2019b) during a field experiment on ship steel coupons exposed in polluted harbour seawater in the Arabian Sea with similar nitrate levels (around 1.5–2 ppm NO_3-N) than those exposed to a natural seawater environment (with no nitrates), for a duration up to a maximum of 112 days. Furthermore, similar corrosion patterns as those resulted in this research in the presence of dissolved nitrates have also been reported by several researchers, however the significant influence nitrates on corrosion has only been recorded during the long-term exposure durations (De Baere et al., 2020; Melchers, 2018, 2014b, 2013a; Wang and Melchers, 2017).

Evidences of accelerated corrosion losses by action of nitrate dosing in offshore steels structures, especially in oxygenated seawater have also been reported by some researchers when used as a biocide for mitigating sour corrosion or MIC (Bødtker et al., 2008; Myhr et al., 2002). Further, nitrate ion at lower concentrations is chemically stable in aqueous systems, it may serve as an excellent oxidising agents (Nemati et al., 2001b). These adverse effects of nitrates in mitigating corrosion losses (sour corrosion led by SRBs) when used as a biocide in offshore oil & gas industry has mainly been attributed to inadequate scavenging of DO, hence complementing the corrosion results presented this paper (conducted in oxygenated artificial seawater rich in nitrates).

Comparative analysis of corrosion products deposited on steel coupons exposed to un-nitrated and nitrated artificial seawater solutions shows visual differences in the texture, type, compactness, and colour of the corrosion product layers accumulated on steel coupons. The corrosion layers deposited on steel coupons (J-series) exposed in nitrated seawater were relatively soft, bright reddish/orange, easily peelable and porous. Such porous corrosion products may provide easy passage for the free movement of aggressive anions from seawater solution to the metal surfaces (Alcántara et al., 2017). On the other hand, similar steel coupons (of C-series) exposed to un-nitrated artificial seawater were observed with distinguished anodic

26

and cathode regions, since the early days of seawater exposure (as shown in Figure 10 and Figure 11, respectively).

Typical rust oxide/hydroxide phases were observed (as shown in Table 1) were observed in SEM micrographs for both types of deposits found on steel coupons exposed to nitrated/nitrated artificial seawater. Relatively higher elemental compositions of S and Cl were observed in corrosion deposits collected from J-series coupons exposed to nitrated seawater (see Table 7 and Table 8). Additionally, SEM micrographs and EDS of protectives deposits appeared on cathode regions of steel plates (C-series) exposed to un-nitrated seawater have shown shapes and compositions altogether different from those appeared on anodic regions, and mainly comprised of Ca, O, and Fe, which probably hints formation of $CaCO_3$ and $FeCO_3$ compounds. These compounds ($CaCO_3$ and $FeCO_3$) typically forms as a protective corrosion deposit on steels exposed to natural seawater with higher alkalinity levels (De Baere et al., 2020; Peng and Park, 1994).

EDS results of corrosion deposits observed on steel coupons exposed to nitrated seawater (in Table 8) show relatively higher levels of S, Cl, and Ca content (wt.%) compared to those corrosion deposits observed in un-nitrated seawater (Table 7). Raman scattering graphs for corrosion products collected from coupons at both exposure conditions have shown strong peaks of typical rust phases, such as goethite, lepidocrocite, magnetite, ferrihydrite, akaganeite and GR (Cl, SO_4) in addition to strong peaks possibly belonging to $CaCO_3$ compounds.

The corrosion losses measured with an unconventional DM-micrometry technique provided more refined and superior quality data, which is otherwise not possible by using traditional mass loss method. This paper demonstrated that a variety of corrosion loss parameters (maximum, mean, cumulative probability, etc.) may be obtained by using the DM-micrometry approach, which can be further utilized in the formulation of corrosion prediction models, remaining useful life prediction modelling, and inspection/maintenance plans for offshore platforms. In fact, this research has shown that the DM-micrometry technique provided a more reliable form of corrosion loss data (both uniform corrosion loss and maximum damage depths), which in turn provides a deeper understanding of the corrosion mechanism(s) taking place in under different exposure conditions and seawater compositions.

This study also suggests that further research would be needed for a greater understanding and improvement in the available knowledge about the complex nexus between dissolved nitrates (DIN compounds) in seawater and the corrosion mechanism in steels, preferably by using

27

various coupon-based corrosion experiments for longer durations, and the electrochemical techniques for instantaneous corrosion measurements. Current research work may be extended in future by carrying out further field/laboratory-based experiments on steels in various seawater exposure conditions, by varying the intensity and proportion of influencing environmental factors including DIN compounds.

5 Conclusion

Corrosion of structural steels exposed to seawater environment is quite complex phenomenon mainly because of the active involvement of numerous factors, variations in chemical constituents as well as environmental factors in seawater. The aim of this paper was to investigate the influence of potassium nitrate, a DIN compound, on the short-term corrosion behaviour of a surface finished steel exposed to an artificial seawater solution at 18 ^{O}C. The conclusions suggestive of the recent knowledge on corrosion mechanism of steel in a nitrated seawater medium can be summarized as follows:

- Corrosion losses and pit depths were observed on steel coupons exposed to nitrated artificial seawater were found to be significantly higher (approximately double) than those resulted on similar coupons subjected to the un-nitrated artificial seawater at that temperature.

- The considerable increase in mean corrosion losses and pit depths observed on coupons exposed to a nitrated seawater affirms that the presence of DIN compound can induce a significant influence on the rate of early corrosion of steels exposed to a synthetic/artificial seawater, which is relatively free from inherent biological constituents.

- The form and texture of the corrosion deposits, surface topologies, formation of distinctive localised anodic/cathode regions, and their adhesion behaviour on the metal surface was quite different in different exposure conditions. In case of un-nitrated seawater exposure conditions, the corrosion products appeared to be highly compact, adherent to surface, clearly distinguished between anode and cathode regions, and hard to remove, therefore, were relatively more protective compared to the non-adherent, porous, uniform, and reddish-brown corrosion products appeared in nitrated seawater solution.

- Corrosion morphologies characterised using SEM and Raman scattering graphs showed typical phases of iron oxides/hydroxides in both exposure conditions, whereas relatively higher S and Cl contents (wt.%) appeared in corrosion deposits extracted from coupons in nitrated seawater. In addition, protective corrosion deposits on cathode regions of steel

28

coupons exposed to un-nitrated seawater resembled the shapes of $CaCO_3$ compounds when seen at a higher magnification under SEM, whereas their elemental compositions in EDS have shown Ca, and O in abundance, which also hints the presence of $CaCO_3$ compounds.

- The DM-micrometry approach used in this paper for measuring the mean corrosion losses and corrosion depths provided a refined and quality data which can be useful in formulation of corrosion prediction models and reliability estimation of off shore platforms.

Conflict of interest statement

No potential conflict of interest was reported by the authors.

Author's contribution

MA performed the experimental work, analytical analysis, and wrote the manuscript text, whereas SR, SS, AR, AK, AL, and AN carried out modifications in paper's structure and revisions.

References

Abbas, M., Mahmood, S., Simms, N., 2019a. Corrosion behaviour of cupronickel 90/10 alloys in Arabian Sea conditions and its effect on maintenance of marine structures, in: Proceedings of the ASME 2019 38th International Conference on Ocean, Offshore and Arctic Engineering. ASME, Glasgow, Scotland, UK, pp. 1–9.

Abbas, M., Simms, N., Lao, L., Malik, O.A., Syed, A.U., Ali Sarfraz, S., Ashraf, L., Rizvi, S.H.M., 2021. A dimensional metrology-based approach for corrosion measurement of ship grade steels exposed to various marine environmental conditions. Corros. Eng. Sci. Technol. 0, 1–13. https://doi.org/10.1080/1478422X.2021.1904096

Abbas, M., Simms, N., Rizvi, S.H.M., 2023. A new approach for quantification of corrosion losses on steels exposed to an artificial seawater environmnet. Corros. J. Sci. Eng. 1–10.

Abbas, M., Simms, N., Syed, A.S., Malik, O.A., Sumner, J., 2019b. Evaluation of the effects of highly saline and warm seawaters on corrosivity of marine assets, in: Eurocorr2019. European Federation of Corrosion, Saville, Spain, pp. 1–14.

Al-Thubaiti, M.A., Hodgkiess, T., Ho, S.Y.K., 2005. Environmental influences on the vapourside corrosion of copper-nickel alloys. Desalination 183, 195–202. https://doi.org/10.1016/j.desal.2005.03.035

Alcántara, J., Chico, B., Simancas, J., Díaz, I., de la Fuente, D., Morcillo, M., 2016. An attempt to classify the morphologies presented by different rust phases formed during the exposure of carbon steel to marine atmospheres. Mater. Charact. 118, 65–78. https://doi.org/10.1016/j.matchar.2016.04.027

Alcántara, J., de la Fuente, D., Chico, B., Simancas, J., Díaz, I., Morcillo, M., 2017. Marine atmospheric corrosion of carbon steel: A review. Materials (Basel). 10. https://doi.org/10.3390/ma10040406

Aromaa, J., Forsén, O., 2016. Factors affecting corrosion in Gulf of Finland brackish water. Int. J. Electrochem. 2016, 1–9. https://doi.org/10.1155/2016/3720280

ASTM G1 − 03, 2017. Standard practice for preparing , cleaning , and evaluating corrosion test. https://doi.org/10.1520/G0001-03R17E01.2

Bødtker, G., Thorstenson, T., Lillebø, B.L.P., Thorbjørnsen, B.E., Ulvøen, R.H., Sunde, E., Torsvik, T., 2008. The effect of long-term nitrate treatment on SRB activity, corrosion rate and bacterial community composition in offshore water injection systems. J. Ind. Microbiol. Biotechnol. 35, 1625–1636. https://doi.org/10.1007/s10295-008-0406-x

Bolwell, R., 2006. Understanding Royal Navy gas turbine sea water lubricating oil cooler failures when caused by microbial induced corrosion ("SRB"). J. Eng. Gas Turbines Power 128, 153–162. https://doi.org/10.1115/1.1926315

Chaves, I.A., Melchers, R.E., 2014. Extreme value analysis for assessing structural reliability of welded offshore steel structures. Struct. Saf. 50, 9–15. https://doi.org/10.1016/j.strusafe.2014.03.007

Coleman, K.E., Simms, N.J., Kilgallon, P.J., Oakey, J.E., 2009. Corrosion in Biomass Combustion Systems. Mater. Sci. Forum 595–598, 377–386. https://doi.org/10.4028/www.scientific.net/msf.595-598.377

Cornell, R.M., Schwertmann, U., 2003. The iron oxides, Second. ed. Wiley-VCH, Weinheim

Germany. https://doi.org/10.1002/3527602097.ch1

De Baere, K., Van Haelst, S., Chaves, I., Luyckx, D., Van Den Bergh, K., Verbeken, K., De Meyer, E., Verhasselt, K., Meskens, R., Potters, G., Melchers, R., 2020. The influence of concretion on the long-term corrosion rate of steel shipwrecks in the Belgian North Sea. Corros. Eng. Sci. Technol. 1–10. https://doi.org/10.1080/1478422X.2020.1807163

de la Fuente, D., Alcántara, J., Chico, B., Díaz, I., Jiménez, J.A., Morcillo, M., 2016a. Characterisation of rust surfaces formed on mild steel exposed to marine atmospheres using XRD and SEM/Micro-Raman techniques. Corros. Sci. 110, 253–264. https://doi.org/10.1016/j.corsci.2016.04.034

de la Fuente, D., Díaz, I., Alcántara, J., Chico, B., Simancas, J., Llorente, I., García-Delgado, A., Jiménez, J.A., Adeva, P., Morcillo, M., 2016b. Corrosion mechanisms of mild steel in chloride-rich atmospheres. Mater. Corros. 67, 227–238. https://doi.org/10.1002/maco.201508488

de la Fuente, D., Díaz, I., Simancas, J., Chico, B., Morcillo, M., 2011. Long-term atmospheric corrosion of mild steel. Corros. Sci. 53, 604–617. https://doi.org/10.1016/j.corsci.2010.10.007

Fanning, J.C., 2000. The chemical reduction of nitrate in aqueous solution. Coord. Chem. Rev. 199, 159–179. https://doi.org/10.1016/s0010-8545(99)00143-5

Fontana, M.G., 1987. Corrosion Engineering, 3rd ed. McGraw Hill Book Company, New York, USA.

Gieg, L.M., Jack, T.R., Foght, J.M., 2011. Biological souring and mitigation in oil reservoirs. Appl. Microbiol. Biotechnol. 92, 263–282. https://doi.org/10.1007/s00253-011-3542-6

Hubert, C., Nemati, M., Jenneman, G., Voordouw, G., 2005. Corrosion risk associated with microbial souring control using nitrate or nitrite. Appl. Microbiol. Biotechnol. 68, 272–282. https://doi.org/10.1007/s00253-005-1897-2

Hubert, C., Nemati, M., Jenneman, G., Voordouw, G., 2003. Containment of biogenic sulphide production in continuous up-flow packed-bed bioreactors with nitrate or nitrite. Biotechnol. Prog. 19, 338–345. https://doi.org/10.1021/bp020128f

Ishikawa, T., Kondo, Y., Yasukawa, A., Kandori, K., 1998. Formation of magnetite in the presence of ferric oxyhydroxides. Corros. Sci. 40, 1239–1251. https://doi.org/10.1016/S0010-938X(98)00045-6

Jeffrey, R., Melchers, R.E., 2009. Effect of vertical length on corrosion of steel in the tidal zone. Corrosion 65, 695–702. https://doi.org/10.5006/1.3319096

Kohn, T., Livi, K.J.T., Roberts, A.L., Vikesland, P.J., 2005. Longevity of granular iron in groundwater treatment processes: Corrosion product development. Environ. Sci. Technol. 39, 2867–2879. https://doi.org/10.1021/es048851k

Kovalenko, R., Melchers, R., Chernov, B., 2017. Long-term immersion corrosion of steel subject to large annual variations in seawater temperature and nutrient concentration. Struct. Infrastruct. Eng. 13, 978–987. https://doi.org/10.1080/15732479.2016.1229797

Li, S., Hihara, L.H., 2015. A Micro-Raman spectroscopic study of marine atmospheric corrosion of carbon steel: The effect of Akaganeite. J. Electrochem. Soc. 162, C495–C502. https://doi.org/10.1149/2.0881509jes

Ma, A.L., Jiang, S.L., Zheng, Y.G., Ke, W., 2015. Corrosion product film formed on the 90/10 copper-nickel tube in natural seawater: composition/structure and formation mechanism. Corros. Sci. 91, 245–261. https://doi.org/10.1016/j.corsci.2014.11.028

Ma, Y., Li, Y., Wang, F., 2008. The effect of β-FeOOH on the corrosion behavior of low carbon steel exposed in tropic marine environment. Mater. Chem. Phys. 112, 844–852. https://doi.org/10.1016/j.matchemphys.2008.06.066

Melchers, 2005. Statistical characterization of pitting corrosion - Part 2: Probabilistic modeling for maximum pit depth. Corrosion 61, 766–777. https://doi.org/10.5006/1.3278211

Melchers, R., 2018. A review of trends for corrosion loss and pit depth in longer-term exposures. Corros. Mater. Degrad. 1, 42–58. https://doi.org/10.3390/cmd1010004

Melchers, R., 2016. Principles of marine corrosion, in: Dhanak, M., Xiros, N.I. (Eds.), Ocean Engineering. Springer, London, pp. 111–123. https://doi.org/10.1007/978-3-319-16649-0_5

Melchers, R., 2014a. Long-term immersion corrosion of steels in seawaters with elevated nutrient concentration. Corros. Sci. 81, 110–116. https://doi.org/10.1016/j.corsci.2013.12.009

Melchers, R., 2014b. Microbiological and abiotic processes in modelling longer-term marine corrosion of steel. Bioelectrochemistry 97, 89–96. https://doi.org/10.1016/j.bioelechem.2013.07.002

Melchers, R., 2013a. Influence of dissolved inorganic nitrogen on accelerated low water corrosion of marine steel piling. Corrosion 69, 95–103. https://doi.org/10.5006/0728

Melchers, R., 2013b. Long-term corrosion of cast irons and steel in marine and atmospheric environments. Corros. Sci. 68, 186–194. https://doi.org/10.1016/j.corsci.2012.11.014

Melchers, R., 2009. Long-term corrosion of steels exposed to marine environments. Eur. J. Environ. Civ. Eng. 13, 527–546. https://doi.org/10.1080/19648189.2009.9693132

Melchers, R., 2007a. Influence of seawater nurtrient content on the early immersion corrosion of mild steel - part 1: empirical observations. Corrosion 63, 318–329. https://doi.org/10.5006/1.3278385

Melchers, R., 2007b. The effects of water pollution on the immersion corrosion of mild and low alloy steels. Corros. Sci. 49, 3149–3167. https://doi.org/10.1016/j.corsci.2007.03.021

Melchers, R., 2006. The marine corrosion of structural steels in brackish and fresh waters. Struct. Infrastruct. Eng. 2, 53–61. https://doi.org/10.1080/15732470500253115

Melchers, R., 2005. Effect of nutrient-based water pollution on the corrosion of mild steel in marine immersion conditions. Corrosion 61, 237–245. https://doi.org/10.5006/1.3280633

Melchers, R., 2003. Mathematical modelling of the diffusion controlled phase in marine immersion corrosion of mild steel. Corros. Sci. 45, 923–940. https://doi.org/10.1016/S0010-938X(02)00208-1

Melchers, R., Chernov, B.B., 2010. Corrosion loss of mild steel in high temperature hard freshwater. Corros. Sci. 52, 449–454.

Melchers, R., Emslie, R., 2016. Investigations for structural safety assessment of corroded cast iron bridge piers. Aust. J. Struct. Eng. 17, 55–66. https://doi.org/10.1080/13287982.2015.1128379

Melchers, R., Jeffrey, R., 2012. Corrosion of long vertical steel strips in the marine tidal zone and implications for ALWC. Corros. Sci. 65, 26–36. https://doi.org/10.1016/j.corsci.2012.07.025

Melchers, R., Jeffrey, R., 2008. Probabilistic models for steel corrosion loss and pitting of marine infrastructure. Reliab. Eng. Syst. Saf. 93, 423–432. https://doi.org/10.1016/j.ress.2006.12.006

Melchers, R., Jeffrey, R.J., 2014. Long-term corrosion of mild steel in natural and uv-treated coastal seawater. Corrosion 70, 804–818. https://doi.org/10.5006/1122

Melchers, R., Wells, T., 2006. Models for the anaerobic phases of marine immersion corrosion. Corros. Sci. 48, 1791–1811. https://doi.org/j.corsci.2005.05.039

Melchers, R.E., 2023. Internal corrosion of parked steel oil pipelines. Ocean Eng. 276, 114145. https://doi.org/10.1016/j.oceaneng.2023.114145

Melchers, R.E., 1999. Corrosion uncertainty modelling for steel structures. J. Constr. Steel Res. 52, 3–19. https://doi.org/10.1016/S0143-974X(99)00010-3

Melchers, R.E., Herron;, C., Emslie, R., 2016. Long term marine corrosion of cast iron bridge piers Long term marine corrosion of cast iron bridge piers. Corros. Eng. Sci. Technol. 51, 248–255. https://doi.org/10.1179/1743278215Y.0000000049

Misawa, T., Hashimoto, K., Shimodaira, S., 1974. The mechanism of formation of iron oxide and oxyhydroxides in aqueous solutions at room temperature. Corros. Sci. 14, 131–149. https://doi.org/10.1016/S0010-938X(74)80051-X

Morcillo, M., Chico, B., de la Fuente, D., Almeida, E., Joseph, G., Rivero, S., Rosales, B., 2004. Atmospheric corrosion of reference metals in Antarctic sites. Cold Reg. Sci. Technol. 40, 165–178. https://doi.org/10.1016/j.coldregions.2004.06.009

Myhr, S., Lillebø, B.L., Sunde, E., Beeder, J., Torsvik, T., 2002. Inhibition of microbial H2S production in an oil reservoir model column by nitrate injection. Appl. Microbiol. Biotechnol. 58, 400–408. https://doi.org/10.1007/s00253-001-0881-8

Nemati, M., Jenneman, G.E., Voordouw, G., 2001a. Impact of nitrate-mediated microbial control of souring in oil reservoirs on the extent of corrosion. Biotechnol. Prog. 17, 852–859. https://doi.org/10.1021/bp010084v

Nemati, M., Jenneman, G.E., Voordouw, G., 2001b. Mechanistic study of microbial control of hydrogen sulfide production in oil reservoirs. Biotechnol. Bioeng. 74, 424–434. https://doi.org/10.1002/bit.1133

Oesch;, S., Heimgartner, P., 1996. Results of an outdoor exposure programme. Mater. Corros. 47, 425–438.

Païssé, S., Ghiglione, J.F., Marty, F., Abbas, B., Gueuné, H., Amaya, J.M.S., Muyzer, G., Quillet, L., 2013. Sulfate-reducing bacteria inhabiting natural corrosion deposits from marine steel structures. Appl. Microbiol. Biotechnol. 97, 7493–7504. https://doi.org/10.1007/s00253-012-4464-7

Paul, S., 2011. Model to study the effect of composition of seawater on the corrosion rate of mild steel and stainless steel. J. Mater. Eng. Perform. 20, 325–334. https://doi.org/10.1007/s11665-010-9686-1

Peng, C.G., Park, J.K., 1994. Principal factors affecting microbiologically influenced corrosion

of carbon steel. Corrosion 50, 669–675. https://doi.org/10.5006/1.3293542

Peng, L., Stewart, M.G., Melchers, R.E., 2017. Corrosion and capacity prediction of marine steel infrastructure under a changing environment. Struct. Infrastruct. Eng. 13, 988–1001. https://doi.org/10.1080/15732479.2016.1229798

Phull, B.S., Pikul, S.J., Kain, R.M., 1997. Seawater corrosivity around the world: results from five years of testing, in: Kian, R.M., T.Young, W. (Eds.), Corrosion Testing in Natural Waters. ASTM International, Norfolk, Virginia, USA, pp. 34–73. https://doi.org/10.1520/STP11357S

Pillay, C., Lin, J., 2014. The impact of additional nitrates in mild steel corrosion in a seawater/sediment system. Corros. Sci. 80, 416–426. https://doi.org/10.1016/j.corsci.2013.11.047

Refait, P., Génin, J.M.R., 1997. The mechanisms of oxidation of ferrous hydroxychloride β-Fe2(OH)3Cl in aqueous solution: The formation of akaganeite vs goethite. Corros. Sci. 39, 539–553. https://doi.org/10.1016/S0010-938X(97)86102-1

Rémazeilles, C., Refait, P., 2007. On the formation of β-FeOOH (akaganéite) in chloride-containing environments. Corros. Sci. 49, 844–857. https://doi.org/10.1016/j.corsci.2006.06.003

Seema Jilani, 2015. Assessment of heavy metal pollution in Lyari river and adjoining coastal areas of Karachi. J. Biodivers. Environ. Sci. 6, 208–214.

Shalaby, H.M., Hasan, A.A., Al-Sabti, F., 2004. Effects of inorganic sulphide and ammonia on microbial corrosion behaviour of 70Cu–30Ni alloy in sea water. Br. Corros. J. 34, 292–298. https://doi.org/10.1179/000705999101500996

Simms, N.J., Oakey, J.E., Nicholls, J.R., 2000. Development and application of a methodology for the measurement of corrosion and erosion damage in laboratory, burner rig and plant environments. Mater. High Temp. 17, 355–362. https://doi.org/10.1179/mht.2000.17.2.025

Smith, M., Bardiau, M., Brennan, R., Burgess, H., Caplin, J., Ray, S., Urios, T., 2019. Accelerated low water corrosion: the microbial sulfur cycle in microcosm. Mater. Degrad. 3, 11. https://doi.org/10.1038/s41529-019-0099-9

Soares, C.G., Garbatov, Y., Zayed, A., 2011. Effect of environmental factors on steel plate corrosion under marine immersion conditions. Corros. Eng. Sci. Technol. 46, 524–541. https://doi.org/10.1179/147842209X12559428167841

Surnam, B.Y.R., Chui, C.W., Xiao, H., Liang, H., 2016. Investigating atmospheric corrosion behavior of carbon steel in coastal regions of Mauritius using Raman Spectroscopy. Rev. Mater. 21, 157–168. https://doi.org/10.1590/S1517-707620160001.0014

Syed, S., 2010. Atmospheric corrosion of carbon steel at marine sites in Saudi Arabia. Mater. Corros. 61, 238–244. https://doi.org/10.1002/maco.200905300

Tanaka, H., Mishima, R., Hatanaka, N., Ishikawa, T., Nakayama, T., 2014. Formation of magnetite rust particles by reacting iron powder with artificial α-, β- and γ-FeOOH in aqueous media. Corros. Sci. 78, 384–387. https://doi.org/10.1016/j.corsci.2013.08.023

Venkatesan, R., Dwarakadasa, E.S., Ravindran, M., 2003. Biofilm formation on structural materials in deep sea environments. Indian J. Eng. Mater. Sci. 10, 486–491.

Wang, X., Melchers, R., 2017. Long-term under-deposit pitting corrosion of carbon steel pipes. Ocean Eng. 133, 231–243. https://doi.org/10.1016/j.oceaneng.2017.02.010

Webster, B.J., Newman, R.C., 1994. Producing rapid Sulfate-Reducing Bacteria (SRB)-influenced corrosion in the laboratory. ASTM-STP1232-EB.

Xu, B., Li, D., Li, W., Xia, S., Lin, Y., Hu, C., 2010. Measurements of dissolved organic nitrogen (DON) in water samples with nanofiltration pretreatment. Water Res. 44, 5376–5384. https://doi.org/10.1016/j.watres.2010.06.034

Xu, D., Li, Y., Song, F., Gu, T., 2013. Laboratory investigation of microbiologically influenced corrosion of C1018 carbon steel by nitrate reducing bacterium Bacillus licheniformis. Corros. Sci. 77, 385–390. https://doi.org/10.1016/j.corsci.2013.07.044

1.

Click here to access/download
Supplementary Material
Supplementary Material- nitrate based corrosion.docx